Technological University Dublin
ARROW@TU Dublin

Articles | Centre for Industrial and Engineering Optics

2004-01-01

Mechancial Characterization of Unplasticised Polyvinylchloride Thick Pipes Using Electronic Speckle Pattern Interferometry

Emilia Mihaylova
Technological University Dublin, emilia.mihaylova@tudublin.ie

Benjamin Potelon
Ecole Nationale D'Ingenieurs de Brest

Guntaka Tulasi Sridhar Reddy
Technological University of Dublin

See next page for additional authors

Follow this and additional works at: https://arrow.tudublin.ie/cieoart

Part of the Electrical and Computer Engineering Commons

Recommended Citation

Mihaylova, E. et al. (2004) Mechancial Characterization of Unplasticised Polyvinylchloride Thick Pipes Using Electronic Speckle Pattern Interferometry. *Optics and Lasers in Engineering*vol. 41, pp.889-900. doi:doi:10.21427/D7T312

This Article is brought to you for free and open access by the Centre for Industrial and Engineering Optics at ARROW@TU Dublin. It has been accepted for inclusion in Articles by an authorized administrator of ARROW@TU Dublin. For more information, please contact arrow.admin@tudublin.ie, aisling.coyne@tudublin.ie, vera.kilshaw@tudublin.ie.

Authors
Emilia Mihaylova, Benjamin Potelon, Guntaka Tulasi Sridhar Reddy, Vincent Toal, and Ciaran Smith

This article is available at ARROW@TU Dublin: https://arrow.tudublin.ie/cieoart/68

MECHANICAL CHARACTERIZATION OF UNPLASTICISED POLYVINYLCHLORIDE THICK PIPES BY OPTICAL METHODS

E. Mihaylova, B. Potelon[1], S. Reddy, V. Toal*, C. Smith[2],
Centre for Industrial and Engineering Optics, School of Physics, Dublin Institute of Technology, Kevin Street, Dublin 8, Ireland
[1]on study leave from Ecole Nationale d'Ingenieurs, Brest, France
[2]Faculty of Engineering, Dublin Institute of Technology
*tel. + 353 1 402 4560   fax + 353 1 402 4988   email: vincent.toal@dit.ie

ABSTRACT

In this work a number of techniques (electronic speckle pattern interferometry, holographic interferometry, strain gauge and finite element method) are brought to bear in order to establish consistency in the results of strain measurement. This is necessary if optical non-destructive testing methods, such as those used here, are to gain acceptance for routine industrial use. The FE model provides a useful check. Furthermore ESPI fringe data facilitates the extension of FE models, an approach that is of growing importance in component testing.

The use of in-plane and out-of-plane sensitive electronic speckle pattern interferometry (ESPI) for non-destructive material characterization of thick unplasticised polyvinylchloride (uPVC) pipes is presented. A test rig has been designed for stressing pipes by internal pressure. ESPI gives a complete mapping of the displacement field over the area imaged by the video camera. The results for the strain of uPVC obtained from ESPI data and from strain gauges are in good agreement. The value of Young's modulus has been obtained from the fringe data and compared with results obtained using holographic interferometry and from strain gauge measurements. The FE model also produces fringe data that is consistent with the ESPI results.

Keywords: strain measurement, electronic speckle pattern interferometry, holographic interferometry

INTRODUCTION

A long-standing engineering problem is the behaviour of thick pipes when mechanical or thermal stress is applied. In certain conditions any existing defect could be significant for the mechanical behaviour of the pipes. For example the working pressure of thick polyvinylchloride pipes used for water transfer is between 9 and 12 bar for different classes of pipes. That is why a quick non-destructive technique for defect detection in such pipes is of great interest to manufacturers.

Optical inspection techniques have three advantages over conventional methods: they are full-field and non-contact in character and may detect a great number of defects. Electronic speckle pattern interferometry, along with other coherent optical techniques, has already been proven to be an effective technique in NDT of materials and components [1-19].

In ESPI [1,2,3] a speckle pattern is formed by illuminating the surface of the object to be tested with laser light. This speckle pattern is imaged onto a CCD array and allowed to interfere with a reference wave, which may or may not be speckled. The resultant speckle interference pattern is transferred to a frame grabber on board a computer, saved in memory, and displayed on a monitor. When the object has been deformed or displaced, the resultant speckle pattern changes owing to the change in path difference between the wave front from the surface and the reference wave. The second resultant speckle pattern is transferred to the computer and subtracted from the stored pattern and the result rectified. The resulting interferogram is displayed on the monitor as a pattern of dark and bright fringes, called correlation fringes. In real time it is possible to grab frames continuously while a deformation is occurring and then subtract them in succession from the first speckle pattern. This process makes it possible to observe the real-time formation and the progressive changes of the fringe pattern related to the deformation of the surface. ESPI detects the deformations in the sub-micrometer range, of the surface of a stressed object. Depending on the design of the interferometer, in-plane sensitivity or out-of–plane sensitivity can be obtained. The fringe pattern on a thick cylinder sample observed near the optical axis of an in-plane sensitive interferometer generally consists of uniform parallel fringes, which increase in spatial frequency as the internal pressure increases. The spacing between neighbouring fringes is inversely proportional to the displacement of the object's surface at any point and therefore characteristic of the strain at the surface of the sample. ESPI is sensitive to extremely small displacements and is therefore ideal for measuring microstrain.

THEORY

1. Interferogram interpretation

The arrangement shown in Fig. 1 produces fringes which are sensitive to in-plane displacement. The spacing between neighbouring fringes is inversely proportional to the displacement and the fringes are aligned perpendicular to the direction of the displacement. Here the object lies in the x,y plane and is illuminated by two plane wavefronts, whose wave front normals lie in the x,z plane at equal and opposite angles, θ, to the surface normal. The centre of the viewing lens aperture lies on the z-axis. When an element is displaced by a distance **d**(d_x, d_y, d_z) the relative phase change between the two beams is given by

$$\Delta\phi = \frac{4\pi}{\lambda} d_x \sin\theta \qquad (1)$$

where λ is the wavelength of the laser. This form of interferometer therefore allows in-plane displacement in the x-direction to be observed independently in the presence of y–displacement and out-of-plane displacements.

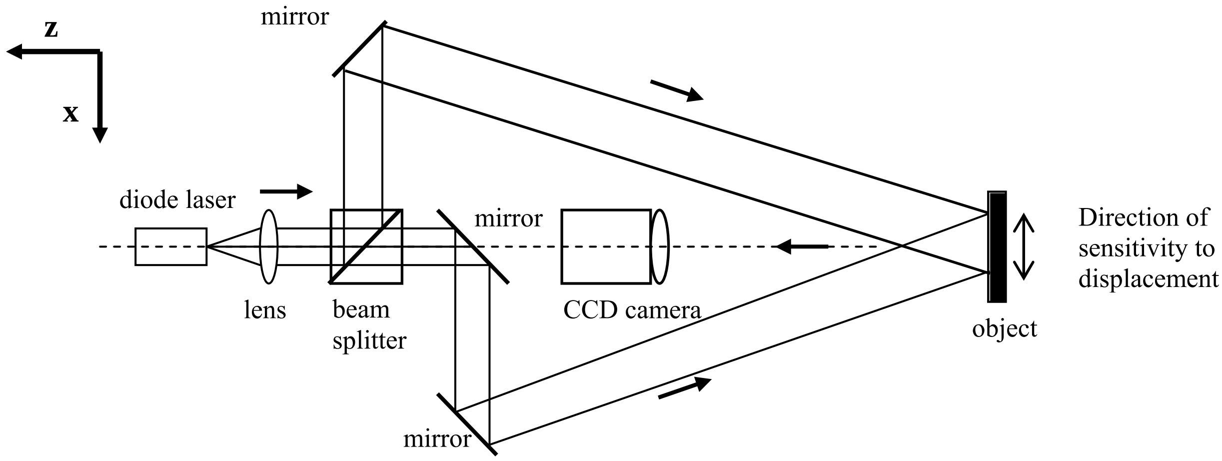

Fig. 1. In-plane sensitive electronic speckle pattern interferometer for the observation of displacement parallel to the x-axis.

An equivalent illumination geometry in which the object is illuminated by beams lying in the y,x plane making equal angles with the z axis will give

$$\Delta\phi = \frac{4\pi}{\lambda} d_y \sin\theta \qquad (2)$$

2. Thick cylinders [20]

For a thick cylinder of internal and external radii subjected to internal pressure *P*, thetangential stress at the outer surface is

$$\sigma_t = \frac{2PR_1^2}{(R_2^2 - R_1^2)} \tag{3}$$

where R_1 and R_2 are the internal and external radii

From equation (1)

$$d_x = \frac{n\lambda}{2\sin\theta} \tag{4}$$

where n is the number of cycles of phase change (fringes) appearing in the field of view *d* (Fig. 2) and d_x is the displacement of a point of the cylinder's surface.

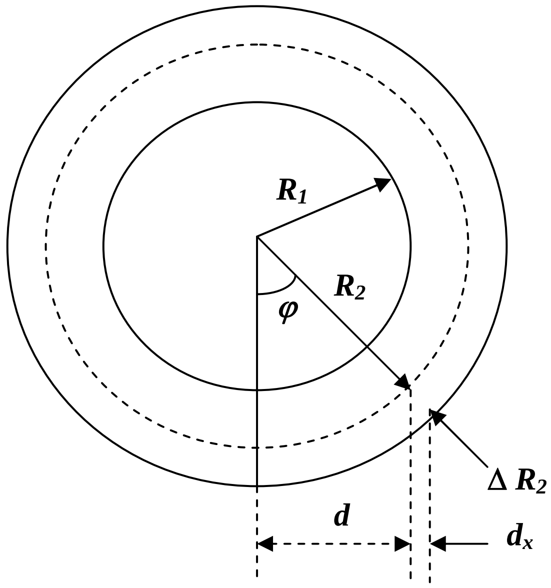

Fig. 2. Effect of cylinder expansion.

$$\sin\varphi = \frac{d}{R_2} = \frac{d_x}{\Delta R_2} \tag{5}$$

From (4) and (5)

$$\Delta R_2 = \frac{d_x}{d} R_2 = \frac{n\lambda}{2\sin\theta}\frac{R_2}{d} \tag{6}$$

and we obtain for the tangential strain

$$\varepsilon_t = \frac{\Delta R_2}{R_2} = \frac{n\lambda}{2d\sin\theta} \tag{7}$$

From thick cylinder theory for a closed cylinder:

$$\sigma_a = (\sigma_r + \sigma_t) / 2 \tag{8}$$

where σ_a, σ_r and σ_t are axial, radial and tangential stresses.

At $r = R_2$, $\sigma_r = 0$ and, from (3)

$$\sigma_t = \frac{2PR_1^2}{(R_2^2 - R_1^2)} \tag{9}$$

Substituting (8) and (9) in (6)

$$\varepsilon_t = \frac{PR_1^2}{(R_2^2 - R_1^2)} \frac{(2-\nu)}{E}, \tag{10}$$

where ν is Poisson's Ratio, which for uPVC is 1/3 and E Young's modulus.

Finally from (7) and (10) we obtain an expression for Young's Modulus:

$$E = \frac{R_1^2}{(R_2^2 - R_1^2)} \frac{2d\sin\theta(2-\nu)}{\lambda} \frac{P}{n} \tag{11}$$

EXPERIMENT

1. The ESPI system

The illuminated object (Fig. 1) is imaged by a CCD camera, which is connected to the frame-grabber. A laser diode, with wavelength 785 nm and a maximum output power of 50 mW, is used as the light source. The beam-splitting unit produces two beams with the same plane of polarisation. The arrangement shown in Fig. 1 gives fringes which are sensitive to in-plane displacement along the x axis. The software [21] controls the frame capture and subtraction operations.

The software also controls the drive current in the laser via a D/A converter connected to the laser power supply. This enables digital phase shifting to be implemented using a 5-bucket algorithm. Four consecutive frames, each phase shifted by 90^0 relative to the preceding one are sufficient to calculate a complete phase map of the speckle interferogram. After the load is applied to the object and a further frame captured the phase map corresponding to the object displacement can be calculated modulo 2π[2]. The map is then unwrapped by working through the image to locate discontinuities in phase and adding or subtracting 2π as appropriate.

2. The sample and test rig

The sample was a thick uPVC cylinder of internal diameter 31.2 cm, external diameter 37.2 cm and length 28.3 cm. Both ends were closed with steel lids (Fig. 3). The cylinder was vertically supported. The pump was attached to a port in the upper lid. The cylinder test rig is intended for use in defect detection. The defects that occur in plastic pipes of this type usually consist of clusters of voids ~ 100 micron in diameter and several cm in length aligned parallel to the axis. One of our research objectives is to devise an inspection method that will detect voids as these may lead to failure under turbulent flow conditions.

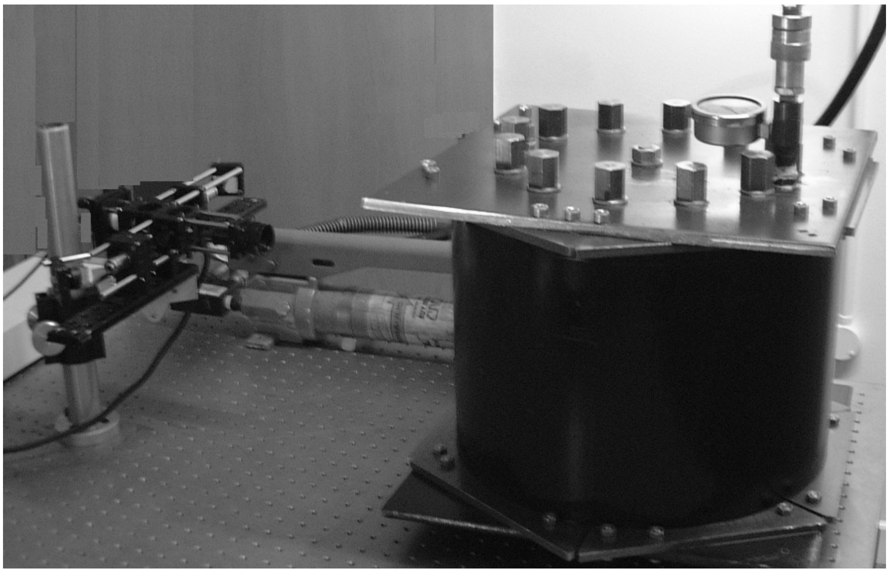

Fig. 3. ESPI system and test cylinder.

3. Experimental procedure

The maximum value of distance d is 4 cm so the focusing error due to the cylinder curvature is very small. ESPI systems involve a small aperture in order to ensure that speckles are resolved. This means that the depth of field is large (ref. 1 page 196) imposing no limitation. The angle θ = arcsin 0.63. The internal pressure applied was in the range 0-2 bar.

RESULTS AND DISCUSSION

1. In-plane ESPI

Fig. 4 shows a typical wrapped phase map produced by a pressure of 2 bar. The area of the cylinder seen here is 1.5 x 1.5 cm^2. Fig. 5 shows the unwrapped phase map and fig. 6, the corresponding in-plane displacement of the cylinder mapped onto 256 gray scale levels (z-axis). The x and y axes are scaled in pixels.

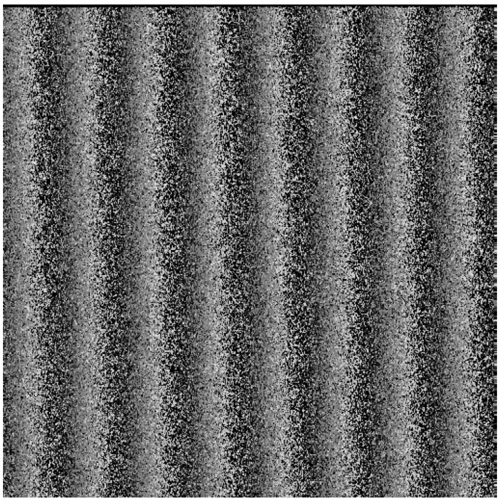

Fig. 4. Wrapped phase map produced by 2 bar pressure.

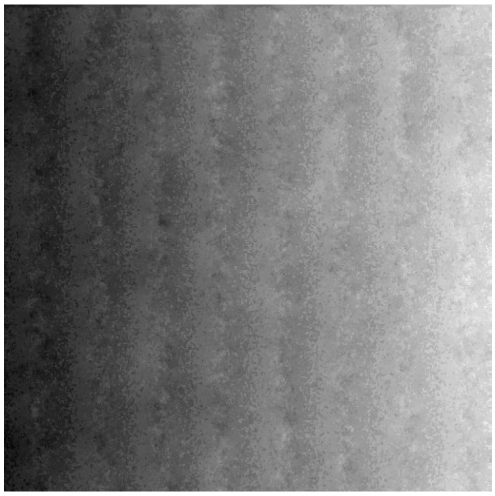

Fig. 5. Unwrapped phase from Fig. 4.

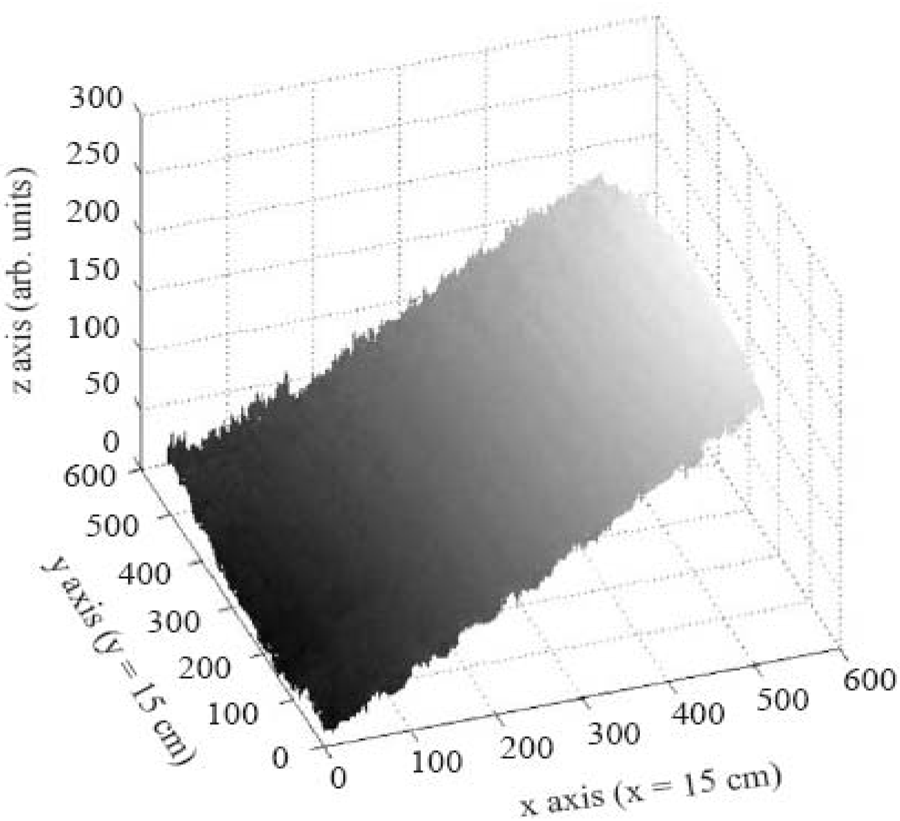

Fig. 6. In-plane displacement of the cylinder at 2 bar.

The results for Young's modulus obtained from ESPI data are given in Table 1

Table 1

Young's modulus for uPVC thick pipes

P (10^5 N m^{-2})	n	E (GN m^{-2})
0.5	5, 5.3, 5, 5	2.6, 2.45, 2.6, 2.6
1	9.5,10, 10, 9.5, 9, 9.5	2.75, 2.6, 2.6, 2.75, 2.9, 2.75
1.5	14.5, 15, 14, 14.5	2.7, 2.6, 2.8, 2.7
2	20, 18.5	2.6, 2.8

For each pressure change P (first column), the number of ESPI fringes due to displacement, n (second column) was noted, each fringe number corresponding to a single experimental trial. The corresponding values of Young's modulus, E, obtained using Eq. (11) are given in column three.

The ESPI derived values for Young's modulus for uPVC material are slightly lower than those quoted by the manufacturer [22] (2.8 - 3.2 GNm^{-2}).

The first experiments gave fringe numbers rather greater than those in the table for the various pressures. A simple analysis of the interferometer geometry shows that for diverging illuminating beams, there is some sensitivity to out-of-plane or radial displacement. This is because the angles of incidence of the two beams are only equal at the centre of the field of view. For example, if the beam cone angle is 10^0 then the angles of incidence will differ by 10^0 at the edge of the field. An out–of–plane displacement d_z will cause an additional optical path change in the interferometer at the edge of the field of view given by

$$d_z(\cos\theta - \cos\theta') \approx d_z(\theta' - \theta)\sin\theta$$

where θ and θ' are the angles of illumination at the edge of the field.

Thus at a pressure of 1 bar we have a radial expansion of about 25 μm giving 2.5 additional fringes. The number increases with pressure leading ultimately to reducing values of E at higher pressures. We cannot remove this error without knowing d_z and the only alternative is to collimate the beams. This was done using achromats of focal length 37.5 cm.

2. Strain gauge measurements

We compared the strain values obtained from ESPI data with measurements using a rosette (0^0, 45^0, 90^0) strain gauge attached to the cylinder and the results, given in Fig. 7, show very good agreement .

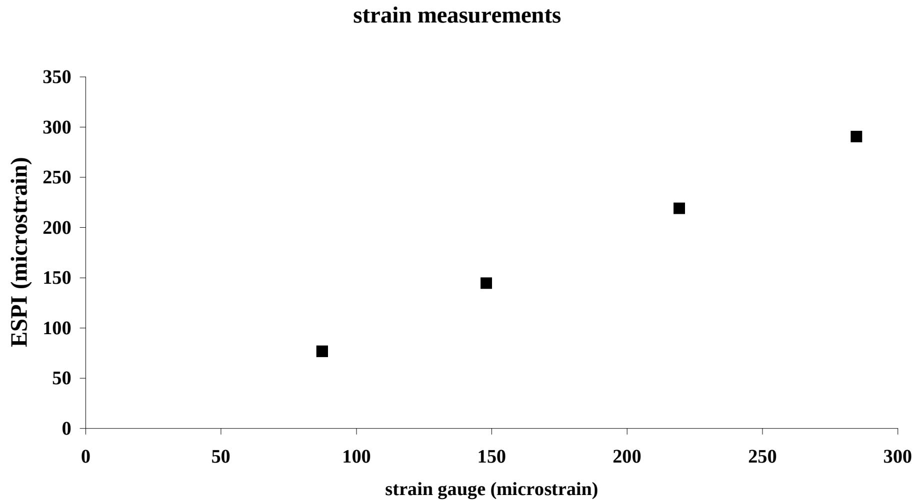

Fig. 7. Strain obtained from ESPI fringes plotted against strain gauge data.

3. Finite element model

We carried out finite element modeling of the pipe using ANSYS5.7 and shell elements. The result for a pressure of 0.5 bar assuming E to be 2.8×10^9 Nm^{-2}, is shown in Fig. 8. This fringe pattern was calculated using MATLAB from the displacement results produced by the finite element model and agrees with the fringe pattern obtained using ESPI at this pressure.

4. Digital Speckle pattern interferometry

By changing the relative phases of the two interfering beams in the interferometer and capturing a new reference frame each time, one can calculate a complete phase map for the reference frame. Then when a frame subtraction is carried out it is possible to obtain the value of the phase difference between the interferograms of the cylinder in unloaded and loaded states. The technique known as digital speckle pattern interferometry. Its use was not required here because of the linearity of the fringe number versus pressure although the fringe number is subject to an error of about 0.5.

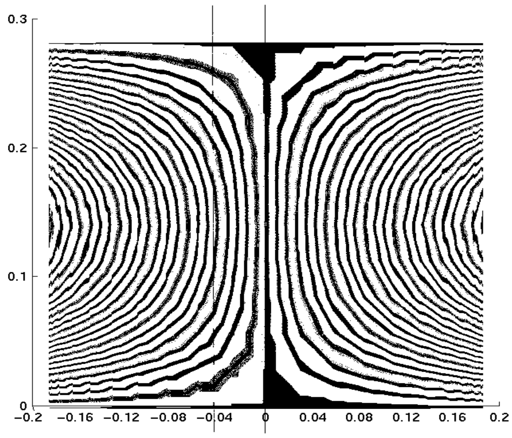

Fig. 8. ANSYS + MATLAB derived fringe pattern for pipe at 0:5 bar pressure. The scales refer to the cylinder dimensions. The fringes are contours of equal displacement in the horizontal direction. Five fringes appear in the region covered by the camera FOV (4 cm) in agreement with the number actually obtained.

5. Out-of-plane sensitivity

Figure 9 shows out-of-plane fringe patterns produced on the surface of uPVC thick pipe by different mechanical stresses. We would expect to observe circular fringes expanding from a point on the sample surface. This is clear when the cylinder is viewed along the horizontal axis of Fig. 8 but the number seen is obviously large even for the case of a very small pressure.

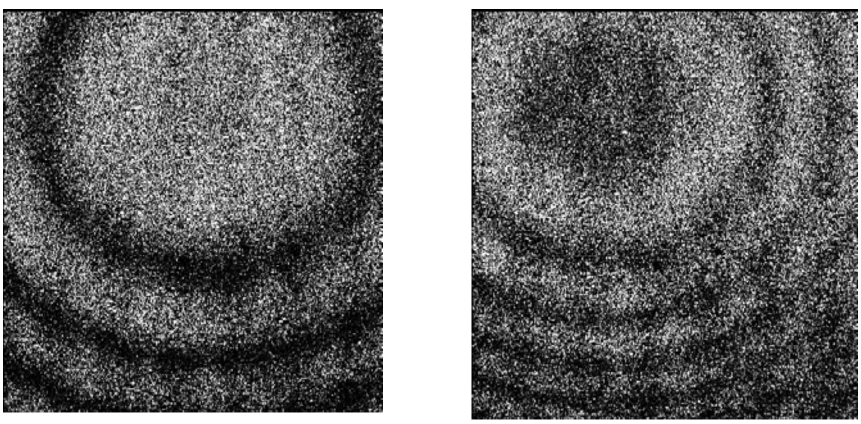

Fig. 9. Out-of-plane displacement fringes at two different pressures.

That is why in-plane ESPI system is more suitable than out-of-plane ESPI system for material testing and defect measurements of thick PVC pipes.

6. Holographic Interferometry

Although out-of-plane ESPI is not a suitable technique for these measurements because of the large numbers of fringes, holographic interferometry can be used with continuous fringe counting. So, as final check on the results of the earlier experiment we recorded a hologram of the cylinder using an Argon ion laser operating at 514 nm and a photopolymer recording material [23,24] developed in our laboratory. The live fringe holographic interferometry method was used to measure the radial expansion of the cylinder and one hundred fringes were counted as the pressure was increased from zero to 1 bar. The illumination and observation directions relative to the cylinder normal, were 20^0 and zero. The radial expansion of the cylinder was found to be 26.5 μm giving 142 μstrain, in agreement with both ESPI and strain gauge results. It was also noted that the fringe count was the same for equal increments in pressure.

CONCLUSIONS

ESPI is an effective non-contact technique for material characterization of thick uPVC pipes. The value of Young's modulus has been obtained from the fringe data using the theory of thick cylinders and it is slightly lower than the expected value, which lies in the range 2.8 – 3.2 GNm^{-2}. The results derived from ESPI data using the theory of thick cylinders and from standard methods agree well with each other. The use of ESPI in material characterization is of interest for industry as a means of optimizing the load bearing characteristics of materials and components. Furthermore, ESPI can be used to detect defects as well as identifying possible failure zones by their anomalous fringe density. The in-plane sensitive ESPI configuration is more suitable than the out-of-plane system for the study of thick pipes. We have shown good agreement between the results obtained using speckle and holographic interferometry and those obtained using conventional methods. Finite element modelling confirms the ESPI results. In summary the work serves to confirm the reliability of the optical techniques used here for material characterization. Future work is aimed at optical detection of voids in thick-walled uPVC pipes.

ACKNOWLEDGMENTS

The authors would like to acknowledge the support of Enterprise Ireland and Wavin Ireland Limited, who jointly funded this research project. Thanks are also due to Henry Rice (Department of Mechanical and Manufacturing Engineering, Trinity College Dublin) for kind assistance with finite element analysis.

REFERENCES

1. Jones R. and Wykes C., Holographic and speckle interferometry, Cambridge University Press: Cambridge 1989
2. Rastogi P. K., Digital speckle pattern interferometry and related techniques, New York: Wiley, 2001
3. Shchepinov V. P. and Pisarev V. S., Stress and strain measurement by holographic and speckle interferometry, Wiley: New York 1996
4. Ravindran V.R., Sarma A.V. and Nayar V.U., Holographic nondestructive testing of low modulus materials, Materials Evaluation, 50, 1058-1065, 1992
5. Chatters T.C., Pouet B.F., Krishnaswamy S., ESPI with synchronized pressure stressing, Proc. SPIE, 1821, 38-45, 1993
6. Garcia G.V., Matthews L., Hickman L., Integration of ESPI and structural analysis to determine the impact of structural defects, Proc. SPIE, 1821, 64-71, 1993
7. Markov V.B., Boone P.M., Burykin N.M., Ovsyannikov V.V., Defect localization in museum items with traditional and electronic holographic nondestructive testing, Proc. SPIE, 2648, 548-556, 1995
8. Jia Z., Shah S., Crack detection in concrete using real-time ESPI technology, Proc. SPIE,. 2455, p. 385-391,, 1995
9. Findeis D.M. and Cryzagoridis J., Inspecting glass fiber reinforced plastic piping using portable ESPI and shearography, 14th World Conference on Nondestructive Testing, New Delhi 8-13 December, 1996
10. Bosco C., Cadoni E., Facchini M., Crack propagation in clay elements determined by ESPI method, Proc. SPIE, 2791, 108-114, 1996
11. Murukeshan V.M., Ganesan A.R. and Sirohi R.S., Design and development of a compact fiber optic phase shifting ESPI system for engineering metrology, 14th World Conference on Nondestructive Testing, New Delhi 8-13 December, 1996
12. Fan H., Song Y., Tan Y., All-optic-fiber phase-shifting ESPI inspection system, Proc. SPIE, 3204, p. 55-60, 1997
13. Cadoni E., Bowe B. and Albrecht D., Application of ESPI technique to evaluate the crack propagation zone of prenotched clay elements, Proc. SPIE, 3407, 410-415, 1998

14. Meinlschmidt P., Bothe T., Hinsch K. and Mehlhorn L., Nondestructive testing and evaluation of historical monuments using thermography and electronic speckle pattern interferometry ESPI, Proc. SPIE, 3396, p. 28-36, 1998

15. Toal V., Martin S. and Bowe B., Non-destructive testing using electronic speckle pattern interferometry, Insight, 41 No 3, 135-140, 1999

16. Petrov V. and Lau B., ESPI with holographically stored waves and other innovative ESPI methods used for real-time monitoring of dynamic thermal deformations in a practical industrial environment, Proc. SPIE, 3824, 262-273, 1999

17. Calvetti F., Cardani G. and Meda A., Mechanical characterization of natural building stones: observation of the fracture process zone by ESPI, Proc. SPIE, 3823, 64-71, 1999

18. Petrov V., Denker R., Lau B., Compact and simple ESPI devices for testing of materials and components in microelectronic manufacturing, Proc. SPIE, 3743, 169-179, 1999

19. Bowe B., Martin S., Toal V., Langhoff A. and Whelan M., Dual in-plane electronic speckle pattern interferometry system with electro-optical switching and phase shifting, Applied Optics, 38, 4, 666-673, 1999

20. Burr A.H. and Cheatham J.B., Mechanical Analysis and Design, London:Prentice Hall, 1995

21. EspiTest software, Copyright © 1999-2000 Andreas Langhoff, Milan, Portions Copyright © European Commission, Joint Research Centre, Ispra, Italy, 1998.

22. Wavinmain Pressure System, Wavin Ireland Limited, Balbriggan, Co. Dublin, Ireland.

22. Martin S., Feely C.A. and Toal V., "Holographic Characteristics of an Acrylamide Based Recording Material", Applied Optics, 36, pp.5757-*5769,* 1997

23. Martin S., Leclere P., Renotte Y., Toal V. and Lion Y., Characterisation of an acrylamide-based dry photopolymer holographic recording material, Optical Engineering, 33, 12, 3942-3946, 1995